

Quantum interferometric power and non-Markovianity in the decoherence channels

Shaojie Xiong(熊少杰), Zhe Sun(孙哲), and Xiaoguang Wang(王晓光)

Citation: Chin. Phys. B, 2023, 32 (**8**): 080302. DOI: 10.1088/1674-1056/accb4e
Journal homepage: http://cpb.iphy.ac.cn; http://iopscience.iop.org/cpb

What follows is a list of articles you may be interested in

Periodic electron oscillation in coupled two-dimensional lattices

Yan-Yan Lu(陆艳艳), Chao Wang(王超), Jin-Yi Jiang(将金益), Jie Liu(刘洁), and Jian-Xin Zhong(钟建新)
Chin. Phys. B, 2023, 32 (**7**): 070306. DOI: 10.1088/1674-1056/acce93

Quantum speed limit of a single atom in a squeezed optical cavity mode

Ya-Jie Ma(马雅洁), Xue-Chen Gao(高雪晨), Shao-Xiong Wu(武少雄), and Chang-Shui Yu(于长水)
Chin. Phys. B, 2023, 32 (**4**): 040308. DOI: 10.1088/1674-1056/acbd2b

Quantum entangled fractional Fourier transform based on the IWOP technique

Ke Zhang(张科), Lan-Lan Li(李兰兰), Pan-Pan Yu(余盼盼), Ying Zhou(周莹),Da-Wei Guo(郭大伟), and Hong-Yi Fan(范洪义)
Chin. Phys. B, 2023, 32 (**4**): 040302. DOI: 10.1088/1674-1056/ac7e32

Floquet scattering through a parity-time symmetric oscillating potential

Xuzhen Cao(曹序桢), Zhaoxin Liang(梁兆新), and Ying Hu(胡颖)
Chin. Phys. B, 2023, 32 (**3**): 030302. DOI: 10.1088/1674-1056/aca39a

Quantum speed-up capacity in different types of quantum channels for two-qubit open systems

Wei Wu(吴薇), Xin Liu(刘辛), Chao Wang(王超)
Chin. Phys. B, 2018, 27 (**6**): 060302. DOI: 10.1088/1674-1056/27/6/060302

Quantum interferometric power and non-Markovianity in the decoherence channels

Shaojie Xiong(熊少杰)[1], Zhe Sun(孙哲)[2,†], and Xiaoguang Wang(王晓光)[3,‡]

[1] *Zhejiang Institute of Modern Physics and Department of Physics, Zhejiang University, Hangzhou* 310027, *China*
[2] *Department of Physics, Hangzhou Normal University, Hangzhou* 310036, *China*
[3] *Key Laboratory of Optical Field Manipulation of Zhejiang Province and Department of Physics, Zhejiang Sci-Tech University, Hangzhou* 310018, *China*

(Received 2 March 2023; revised manuscript received 5 April 2023; accepted manuscript online 7 April 2023)

In quantum open systems, non-Markovianity is an important phenomenon that allows a backflow of information from the environment to the system. In this work, we investigate the non-Markovianity problems in two different types of channels, where the system–environment interactions are treated with and without the rotating-wave approximation (RWA). We employ the quantum interferometric power (QIP) to quantify the non-Markovian dynamics, which is the minimal quantum Fisher information obtained by the local unitary evolution in a bipartite system. By the hierarchy equation method, we calculate the dynamical evolution of the QIP in the non-RWA case. The results show that the dynamical behavior under the non-RWA is significantly different from that under the RWA in both weak and strong coupling. Moreover, in the non-RWA case, we also find the nonmonotonic behavior of the non-Markovianity measure with the variation of coupling strength, which is caused by the competition between the rotating-wave terms and the counterrotating-wave terms. As a result, we highlight the importance of the counterrotating-wave terms for the influence of non-Markovianity.

Keywords: quantum open system, auantum non-Markovianity, auantum interferometric power

PACS: 03.65.–w, 05.30.–d, 03.65.Yz **DOI:** 10.1088/1674-1056/accb4e

1. Introduction

In realistic quantum processes, a quantum system is generally considered as an open quantum system since it unavoidably interacts with its environment. The decoherence caused by system-environment interactions is one of the huge challenges in the implementation of quantum information processing. For weak system–environment coupling and short environment correlation time, the dynamics of an open system can be studied by the Markovian approximation, which neglects the memory effects of the environment. However, the Markovian approximation can not optimally describe most open quantum systems in the strong coupling regime, which are non-Markovian.[1–3] Moreover, non-Markovian dynamics allows a backflow of information from the environment to the system, which leads to a recovery of quantum features, such as the phenomenon of entanglement from disappearance to recovery.[4,5] Non-Markovianity is a useful complement to the basic theory of quantum mechanics and has many applications in dealing with the complex dynamics of open systems,[6] such as chaotic systems,[7] optomechanical systems,[8] and waveguide quantum electrodynamics systems.[9] To quantify non-Markovianity, many measures and witnesses have been proposed based on the trace distance of quantum states,[10] quantum entanglement,[11,12] quantum fidelity,[13] quantum coherence,[14] quantum Fisher information flow,[15] quantum mutual information flow,[16] and relative entropy.[17] Importantly, non-Markovian dynamics has been successfully observed in many experiments.[18–21]

In Ref. [22], the authors first proposed the concept of quantum interferometric power (QIP), which is defined by the minimal quantum Fisher information obtained by the local unitary evolution in a bipartite system. The QIP is a useful theoretical tool that can be applied to quantify discord-like quantum correlations. Then, the QIP was employed to characterize the non-Markovianity of the open system in a local decoherence channel,[23] where the Hamiltonian can be modeled by the interaction between a qubit system and a thermal reservoir under the rotating-wave approximation (RWA), i.e, the so-called Jaynes–Cummings (JC)-type interaction. However, the RWA description for an open quantum system is only acceptable under the weak-coupling condition. With the increase of coupling, the counterrotating terms in the non-RWA may lead to conclusions quite different from the RWA cases.[24] For example, the effect of counterrotating terms has been found to play a significant role in characterizing the two-stage Landau–Zener transition,[25] the quantum Zeno phenomenon for a hydrogen in free space,[26] the temporal quantum steering behavior[27] and the absence of vacuum-induced Berry phases.[28]

In this work, we study the influence of the non-RWA decoherence channel on the dynamical evolution of QIP. To calculate the dynamics under the non-RWA channel, we use the hierarchy equation method introduced in Refs. [29,30].

†Corresponding author. E-mail: sunzhe@hznu.edu.cn
‡Corresponding author. E-mail: xgwang@zstu.edu.cn

© 2023 Chinese Physical Society and IOP Publishing Ltd

In this method, all orders of system–environment interactions are included and the limitations caused by the Born, Markov, and rotating-wave approximation are avoided. This method has been successfully employed to exactly describe the open-system dynamics in many physical systems, chemical systems and quantum devices.[31,32] Our results demonstrate the different dynamics of QIP under the non-RWA channel and the RWA channel. In addition, we also calculate the quantification of non-Markovianity in terms of QIP under the two decoherence channels and show how the counterrotating terms impact the non-Markovian effect of the system.

2. Theoretical method

2.1. The non-Markovianity measure based on QIP

Let us introduce the black box parameter estimation task (see the scheme in Fig. 1). A bipartite ρ_{ab} is shared by Alice and Bob. On Bob's side, there is an unknown parameter θ introduced by a black box device. The operation in the black box is a local unitary evolution $U=\exp(-\mathrm{i}\theta I_a\otimes H_b)$, where I_a is the identity operator acting on a, and H_b is the local Hamiltonian acting on b. After the transformation, Alice and Bob perform the optimal joint measurement on the final state ρ_{ab}^{θ} to estimate θ. According to the quantum Cramér–Rao inequality,[33,34] the lower-bound of variance of the unbiased estimator θ_{est} is bounded by quantum Fisher information (QFI), which is defined as[35,36]

$$\mathcal{F}(\rho_{ab}^{\theta},H_b)=4\sum_{m,n}\frac{(\lambda_m-\lambda_n)^2}{\lambda_m+\lambda_n}|\langle\chi_m|I_a\otimes H_b|\chi_n\rangle|^2, \quad (1)$$

where $\rho_{ab}^{\theta}=\sum_n\lambda_n|\chi_n\rangle\langle\chi_n|$ is the spectral decomposition, and $\lambda_n+\lambda_m>0$. The minimum QFI over all H_b with nondegenerate is defined as the QIP ($\mathcal{Q}$), which is[22]

$$\mathcal{Q}(\rho_{ab}^{\theta})=\frac{1}{4}\inf_{H_b}\mathcal{F}(\rho_{ab}^{\theta},H_b), \quad (2)$$

where 1/4 is a convenient normalization. Consider that the subsystem b is a qubit system and the local Hamiltonian can be written as $H_b=\boldsymbol{r}\cdot\boldsymbol{\sigma}$, with $\boldsymbol{r}=(r_1,r_2,r_3)$ being the Bloch vector and $\boldsymbol{\sigma}=(\sigma_x,\sigma_y,\sigma_z)$ the vector of Pauli matrices. Under the special conditions, the QIP in Eq. (2) is given by the analytic expression[22]

$$\mathcal{Q}(\rho_{ab}^{\theta})=1-G_k^{\max}, \quad (3)$$

where $G_k^{\max}$ is the maximum eigenvalue of the matrix K with elements

$$K_{ij}=\sum_{m,n}\frac{2\lambda_n\lambda_m}{\lambda_n+\lambda_m}\langle\chi_m|I_a\otimes\sigma_b^i|\chi_n\rangle\langle\chi_n|I_a\otimes\sigma_b^j|\chi_m\rangle. \quad (4)$$

For a general quantum state ρ_{ab}, the QIP is a computable measure of discord-type quantum correlations.[22] More importantly, the value of QIP is monotonically decreasing under arbitrary local completely positive and trace preserving (CPTP) maps [denoted by $M_a(t)$] acting on the system a. The composite dynamics of the bipartite system under the local map $M_a(t)$ can be written as

$$\rho_{ab}(t)=(M_a(t)\otimes I_b)\rho_{ab}(0), \quad (5)$$

where I_b is the identity operator acting on b. For all dynamical semigroups and all time-dependent Markovian processes, $M_a(t)$ is a divisible CPTP map and QIP satisfies $\mathrm{d}\mathcal{Q}(\rho_{ab}^{\theta}(t))/\mathrm{d}t\le 0$ for $t\ge 0$ and any initial states.[23] Therefore, if there exist an initial state and a certain time interval such that $\mathrm{d}\mathcal{Q}(\rho_{ab}^{\theta}(t))/\mathrm{d}t>0$, non-Markovianity will appear. The quantification of non-Markovianity based on the QIP is defined as[23]

$$\mathcal{N}_{\mathcal{Q}}(M_a)=\max_{\rho_{ab}(0)}\int_{D(t)>0}D(t)\mathrm{d}t, \quad (6)$$

where $D(t)=\mathrm{d}\mathcal{Q}(\rho_{ab}^{\theta}(t))/\mathrm{d}t$, and the maximum is taken over all sets of possible initial system $\rho_{ab}(0)$. However, the maximization in the measure of Eq. (6) is hardly achievable by finding the optimal state. Instead, we choose the maximum entangled state as the initial state, i.e., $\rho_{ab}(0)=|\Psi\rangle\langle\Psi|$, $|\Psi\rangle=1/\sqrt{2}(|00\rangle+|11\rangle)$. At least in this special initial state, the partial non-Markovianity of the system dynamics can be reflected. In addition, to emphasize the impact of the counterrotating-wave terms, it is better to consider the same initial states and to analyze the different non-Markovian dynamics between the RWA and non-RWA cases.

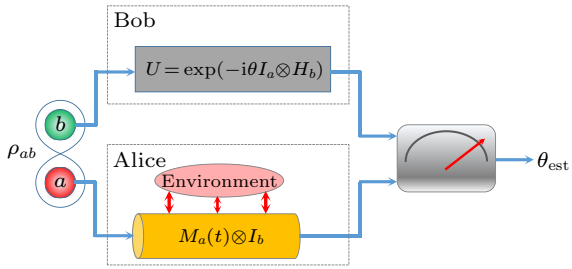


Fig. 1. The diagram shows the black box quantum estimation task. The system a couples with a local environment, and a local unitary evolution U acts on the system b.

2.2. RWA channel and non-RWA channel

The composite dynamical map is $\rho_{ab}(t)=(M_a(t)\otimes I_b)|\Psi\rangle\langle\Psi|$. We first consider that $M_a(t)$ is the single-qubit non-RWA channel, which can be modeled by a qubit system interacting with a bosonic bath. The Hamiltonian can be described as

$$H=\frac{\omega_0}{2}\sigma_z+\sum_k\omega_k a^{\dagger}a+\sum_k(\sigma_+ +\sigma_-)(g_k a_k+g_k^{*}a_k^{\dagger}), \quad (7)$$

where σ_z is the Pauli-Z operator, ω_0 is the transition frequency of the qubit system, $a^{\dagger}$ (a) is the the bosonic creation (annihilation) operator of the k-th mode of the frequency ω_k, σ_+ (σ_-) is the raising (lowering) Pauli operator, g_k is the coupling

strength between the qubit and the k-th mode of the environment. When the RWA is applicable, the Hamiltonian becomes

$$H_{\rm RWA}=\frac{\omega_0}{2}\sigma_z+\sum_k\omega_k a^\dagger a+\sum_k(g_k a_k\sigma_+ + g_k^* a_k^\dagger\sigma_-), \quad (8)$$

where the counterrotating terms $g_k a_k\sigma_-$ and $g_k^* a_k^\dagger\sigma_+$ are omitted when $\omega_0+\omega_k \gg |g_k|$. The counterrotating terms can cause double excitation of the system and environment, i.e., it can drive the system to jump from the low energy state to the high energy state and emit a photon. To understand the physical nature of double excitation process, it is generally accepted that the absorption and emission of photons are virtual processes (very short-lived photons).

Consider that the system a and the environment are initially in $\rho_a(0)\otimes|{\rm vac}\rangle\langle{\rm vac}|$, where the environment is in the vacuum state $|{\rm vac}\rangle\equiv\otimes_k|0\rangle_k$. The system-environment coupling spectrum is assumed to be a Lorentzian broadening with

$$J(\omega)=\frac{1}{2\pi}\frac{\gamma\lambda^2}{(\omega-\omega_0)^2+\lambda^2}, \quad (9)$$

where λ is the spectral width of the coupling, γ is the system-environment coupling constant. The effective coupling can be obtained as $g_{\rm eff}^2=\frac{1}{2}\lambda\gamma$ by integrating $J(\omega)$ over the entire region of ω.

Under the Hamiltonian $H_{\rm RWA}$, the dynamical map of system a can be described as

$$M_a(t)\rho_a(0)=\begin{bmatrix}\rho_{a00}(0)+\rho_{a11}(0)(1-P^2) & \rho_{a01}(0)P\\ \rho_{a10}(0)P^* & \rho_{a11}(0)P^2\end{bmatrix}, \quad (10)$$

where $\rho_{ai,j}(0)$ is the matrix element of the initial state, P is the function of evolution time t and coupling strength g_k. For convenience, we call the decoherence process in Eq. (10) as the RWA channel. For the Lorentzian spectral distribution in Eq. (9), the analytical result of parameter P reads[37]

$$P=\mathrm{e}^{\frac{-\lambda t}{2}}\left[\cosh\left(\frac{dt}{2}\right)+\frac{\lambda}{d}\sinh\left(\frac{dt}{2}\right)\right], \quad (11)$$

where $d=\sqrt{\lambda^2-2\gamma\lambda}$. Under the Hamiltonian H in Eq. (7), the analytical result of the system dynamical map is difficult to obtain. To solve this problem, we employ the hierarchy equation method to calculate the dynamical map of the non-RWA channel, which is shown in Appendix A.

3. Results and discussion

Figure 2(a) shows $\mathcal{Q}(\rho_{ab}^\theta(t))$ versus scaled time $\omega_0 t$ in the RWA and non-RWA channels. The parameters of the coupling spectrum are chosen as $\gamma=0.06\omega_0$ and $\lambda=0.2\omega_0$, i.e., $\gamma/\lambda=3/10$, which is a weak-coupling case. The monotonic decreasing behavior of $\mathcal{Q}(\rho_{ab}^\theta(t))$ appears in the RWA and non-RWA channels. Although in the weak coupling region, the dynamic behavior of $\mathcal{Q}(\rho_{ab}^\theta(t))$ under the two channels is different, where $\mathcal{Q}(\rho_{ab}^\theta(t))$ in the non-RWA channel present more frequent oscillations compared with the situations in the RWA channel. To demonstrate the differences between the two channels more clearly, we plot $D(t)$ versus scaled time $\omega_0 t$ in Fig. 2(b), where the oscillating behavior in the non-RWA channel can be obviously found. However, $D(t)$ is always less than zero in the two channels.

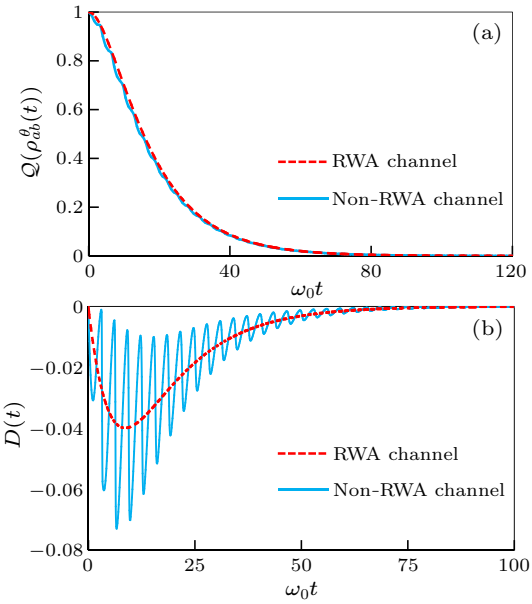


Fig. 2. The $\mathcal{Q}(\rho_{ab}^\theta(t))$ (a) and $D(t)$ (b) versus scaled time $\omega_0 t$ in the two types of channels for $\gamma=0.06\omega_0$ and $\lambda=0.2\omega_0$.

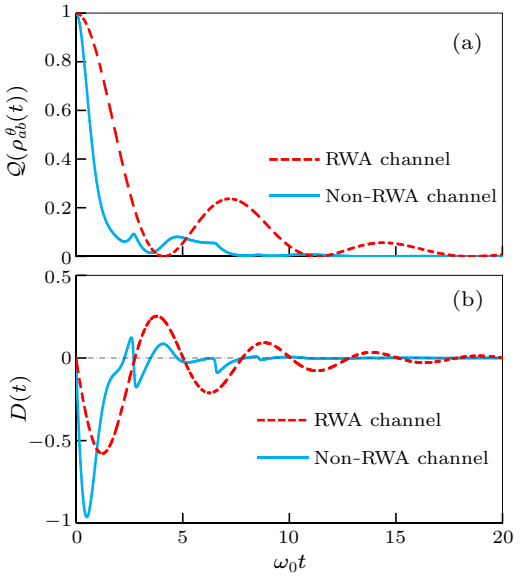


Fig. 3. The $\mathcal{Q}(\rho_{ab}^\theta(t))$ (a) and $D(t)$ (b) versus scaled time $\omega_0 t$ in the two types of channels for $\gamma=2\omega_0$ and $\lambda=0.2\omega_0$.

The strong-coupling case $\gamma/\lambda>0.5$ is shown for $\gamma=2\omega_0$ and $\lambda=0.2\omega_0$ in Fig. 3(a). In the considered region of the coupling parameters, the dynamic evolution of $\mathcal{Q}(\rho_{ab}^\theta(t))$ in the two channels is nonmonotonic, which indicates the existence of non-Markovianity. The difference is that the values of $\mathcal{Q}(\rho_{ab}^\theta(t))$ decay to zero more quickly in the non-RWA channel than that in the RWA channel. The increase of amplitude of $\mathcal{Q}(\rho_{ab}^\theta(t))$ in the RWA channel is obviously greater than that

in the non-RWA channel, which causes the sum of the regions of $D(t) > 0$ to be also larger in Fig. 3(b).

To investigate the differences of non-Markovianity between the two channels, we calculate the non-Markovianity measure $\mathcal{N}_\mathcal{Q}$, integrating over all increasing regions of $\mathcal{Q}(\rho_{ab}^{\theta}(t))$, versus different coupling parameters γ in Fig. 4(a). For the RWA channel, λ and γ are connected to the environment correlation time τ_B and the relaxation time τ_S respectively, i.e., $\tau_\mathrm{B} \sim \lambda^{-1}$ and $\tau_\mathrm{S} \sim \gamma^{-1}$. This implies that the non-Markovian effect will become increasingly strong with the increase of γ/λ. Undoubtedly, we can find that $\mathcal{N}_\mathcal{Q}$ in the RWA channel rises continuously with the increase of coupling strength γ. However, different from the continuous rise of $\mathcal{N}_\mathcal{Q}$ in the RWA channel, an obviously nonmonotonic behavior of $\mathcal{N}_\mathcal{Q}$ on γ is presented in the non-RWA case. With the increase of γ, $\mathcal{N}_\mathcal{Q}$ in the non-RWA channel rises at first and then reaches a maximum value, and finally decays gradually.

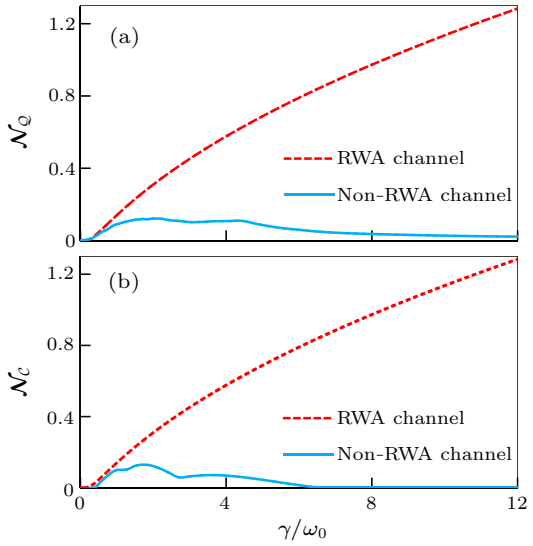


Fig. 4. Non-Markovianity measure $\mathcal{N}_\mathcal{Q}$ (a) and $\mathcal{N}_\mathcal{C}$ (b) versus the coupling parameter γ. The spectral width is $\lambda = 0.2\omega_0$. The integration time is long enough until $D(t)$ converges to 0.

To compare other non-Markovian measures, we show the measure of non-Markovianity based on quantum entanglement (denoted by $\mathcal{N}_\mathcal{C}$)[12] in Fig. 4(b), where the quantum concurrence is chosen as the measure of entanglement.[38] We can observe that the behavior of $\mathcal{N}_\mathcal{C}$ in the RWA channel is similar to that of $\mathcal{N}_\mathcal{Q}$. However, in the non-RWA channel, the zero value of $\mathcal{N}_\mathcal{C}$ appears in the region of $\gamma/\omega_0 > 6.3$, whereas $\mathcal{N}_\mathcal{Q}$ does not decay to zero in the same region. This is because the QIP is a measure of quantum discord, which is a bipartite quantum correlation beyond entanglement.[39] In addition, the values of $\mathcal{N}_\mathcal{Q}$ and $\mathcal{N}_\mathcal{C}$ in the RWA channel are always greater than the situation in the non-RWA channel with the same coupling parameters, which implies that considering the effect of the counterrotating-wave terms in the presence of rotating-wave terms can reduce the non-Markovianity. This is because the conservation of the excitation number between the system and the environment is broken when the counterrotating-wave terms are considered. The multiple excitation mechanism can inhibit the flow of information from the environment to the system.

There are two mechanisms influencing the open system under the non-RWA channel, which are the conservation of the total system-environment excitation number caused by the rotating-wave terms in the interaction Hamiltonian and the double excitations of the system-environment space and multimode excitations of the environment caused by the counterrotating-wave terms. The non-Markovian behavior of the system evolution relies on the two mechanisms. When the coupling constant γ is changed as a single variable, the competition between the two mechanisms can cause the nonmonotonic behavior of the non-Markovianity.

4. Conclusion

Using the hierarchy equation method, we have investigated the problem of non-Markovianity in the non-RWA quantum channel. The numerical results show quite different behaviors of the QIP and the non-Markovianity measure in the RWA and non-RWA cases. Particularly, the dynamic behavior of QIP in the non-RWA case exhibits more frequent oscillations than that in the RWA case. Furthermore, in the non-RWA case, the non-Markovian measure has a significant nonmonotonic dependence on the coupling parameter, which cannot be found in the RWA case. We propose that this nonmonotonicity is caused by the competition between the mechanisms of the conservation excitation (induced by rotating-wave terms) and the double excitation (induced by counterrotating-wave terms). Compared with the non-Markovian measure based on the quantum concurrence, the non-Markovian measure based on the QIP has obvious advantages in the non-RWA channel. Our results reveal the importance of counterrotating-wave terms in research of non-Markovianity.

Appendix A: Hierarchy equation method

For the system-environment Hamiltonian in Eq. (7), the dynamics of the system in the interaction picture can be written as

$$\rho_{ab}(t) = \mathcal{T}\exp\left(-\int_0^t \mathrm{d}t_2 \int_0^{t_2} \mathrm{d}t_1 V^{\times}(t_2)[C_\mathrm{R}(t_2-t_1)V^{\times}(t_1) + \mathrm{i}C_\mathrm{I}(t_2-t_1)V^{\circ}(t_1)]\right)\rho_{ab}(0), \tag{A1}$$

where $A^{\times}B \equiv [A,B] = AB - BA$ and $A^{\circ}B \equiv \{A,B\} = AB + BA$, V is the operator of the qubit in the interaction Hamiltonian, $\mathcal{T}$ is the chronological time ordering operator. The initial state of qubit and environment is $\rho(0) = \rho_{ab}(0) \otimes \rho_\mathrm{E}$, where ρ_E is the initial state of the environment. $C_\mathrm{R}(t_2 - t_1)$

and $C_{\rm I}(t_2-t_1)$ are the real and imaginary parts of the environment time-correlation function $C(t_2-t_1)\equiv\langle B(t_2)B(t_1)\rangle = {\rm Tr}[B(t_2)B(t_1)\rho_E]$, respectively, with $B(t)=\sum_k(g_k a_k\,{\rm e}^{-{\rm i}\omega_k t}+g_k^* a_k^\dagger\,{\rm e}^{{\rm i}\omega_k t})$.

It is difficult to solve Eq. (A1) analytically because of the time-ordered integral. We employ the hierarchy equation method to deal with this problem, which requires solving a set of hierarchy equations.[29,30]

To derive the hierarchy equation, the correlation function $C(t_2-t_1)$ must be decomposed into a sum of exponential functions of time as $C(t_2-t_1)=\sum_k f_k\exp(-\gamma_k)$, where f_k and γ_k depend on the system-environment coupling spectrum and the temperature. Then, the hierarchy equations are obtained by repeatedly taking the derivative of the right-hand side. For the zero temperature case, i.e., $\rho_{\rm E}=\otimes_k|0\rangle_k$, the coupling spectrum can be considered as a Lorentzian type

$$J(\omega)=\frac{1}{2\pi}\frac{\gamma\lambda^2}{(\omega-\omega_0)+\lambda^2}. \tag{A2}$$

Thus, the time-correlation function is

$$C(t_2-t_1)=\frac{1}{2}\gamma\lambda\exp\Big[-(\lambda+{\rm i}\omega_0|t_2-t_1|)\Big]. \tag{A3}$$

This exponential form is necessary for the hierarchy equations. Then, the real and imaginary parts of the time-correlation function $C(t_2-t_1)$ can be written as

$$C_{\rm R}(t)=\sum_{k=1}^{2}\frac{\gamma\lambda}{4}{\rm e}^{-\nu_k t},\quad C_{\rm I}(t)=\sum_{k=1}^{2}(-1)^k\frac{\gamma\lambda}{4{\rm i}}{\rm e}^{-\nu_k t}, \tag{A4}$$

where $\nu_k=\lambda+(-1)^k{\rm i}\omega_0$. According to the procedure shown in Refs. [29,30], the hierarchy equations are obtained as follows:

$$\begin{aligned}\frac{\partial}{\partial t}\rho_{\boldsymbol{n}}(t)=&-({\rm i}H_{\rm s}^{\times}+\boldsymbol{n}\cdot\boldsymbol{\nu})\rho_{\boldsymbol{n}}(t)-{\rm i}\sum_{k=1}^{2}V^{\times}\rho_{\boldsymbol{n}+\boldsymbol{e}_k}(t)\\&-{\rm i}\frac{\gamma\lambda}{4}\sum_{k=1}^{2}n_k\Big[V^{\times}+(-1)^k V^{\circ}\Big]\rho_{\boldsymbol{n}-\boldsymbol{e}_k}(t),\end{aligned} \tag{A5}$$

where the subscript $\boldsymbol{n}=(n_1,n_2)$ is a two-dimensional index with integer numbers $n_{1(2)}\geq 0$, and $\rho_{ab}(t)\equiv\rho_{0,0}(t)$. The vectors $\boldsymbol{e}_1$ and $\boldsymbol{e}_2$ are $\boldsymbol{e}_1=(1,0)$ and $\boldsymbol{e}_2=(0,1)$, and $\boldsymbol{\nu}=(\nu_1,\nu_2)=(\lambda-{\rm i}\omega_0,\lambda+{\rm i}\omega_0)$. Note that $\rho_{\boldsymbol{n}}(t)$ with $\boldsymbol{n}\neq(0,0)$ are auxiliary operators introduced only for the sake of computing, they are not density matrices and are all set to be zero at $t=0$. The hierarchy equations are a set of linear differential equations and can be solved using the Runge–Kutta method.

Acknowledgments

This work was supported by the National Natural Science Foundation of China (Grant Nos. 11935012, 12175052, and 11775065) and the Postdoctoral Science Foundation of China (Grant No. 2022M722794).

References

[1] Breuer H P and Petruccione F 2002 *The Theory of Open Quantum Systems* (New York: Oxford University Press)
[2] Vega I de and Alonso D 2017 *Rev. Mod. Phys.* **89** 015001
[3] Breuer H P, Laine E M, Piilo J and Vacchini B 2016 *Rev. Mod. Phys.* **88** 021002
[4] Xu J S, Li C F, Gong M, Zou X B, Shi C H, Chen G and Guo G C 2010 *Phys. Rev. Lett.* **104** 100502
[5] Fanchini F F, Karpat G, Cakmak B, Castelano L K, Aguilar G H, Farías O J, Walborn S P, Souto Ribeiro P H and de Oliveira M C 2014 *Phys. Rev. Lett.* **112** 210402
[6] Munsif J, Xu X Y, Wang Q Q, Chen Z, Han Y J, Li C F and Guo G C 2019 *Chin. Phys. B* **28** 090303
[7] Žnidarič M, Pineda C and García-Mata I 2011 *Phys. Rev. Lett.* **107** 080404
[8] Mazzola L, Laine E M, Breuer H P, Maniscalco S and Piilo J 2010 *Phys. Rev. A* **81** 062120
[9] Zeng J, Song Y J, Lu J and Zhou L 2023 *Chin. Phys. B* **32** 030305
[10] Breuer H P, Laine E M and Piilo J 2009 *Phys. Rev. Lett.* **103** 210401
[11] Rivas Á, Huelga S F and Plenio M B 2010 *Phys. Rev. Lett.* **105** 050403
[12] Bellomo B, Lo Franco R and Compagno G 2007 *Phys. Rev. Lett.* **99** 160502
[13] Rajagopal A K, Usha Devi A R and Rendell R W 2010 *Phys. Rev. A* **82** 042107
[14] Wu D K, Hou Z B, Xiang G Y, Li C F, Guo G C, Dong D Y and Nori F 2020 *npj Quantum Inf.* **6** 55
[15] Lu X M, Wang X and Sun C P 2010 *Phys. Rev. A* **82** 042103
[16] Luo S, Fu S and Song H 2012 *Phys. Rev. A* **86** 044101
[17] Luo Y and Li Y M 2019 *Chin. Phys. B* **28** 040301
[18] Li C F, Tang J S, Li Y L and Guo G C 2011 *Phys. Rev. A* **83** 064102
[19] Liu B H, Li L, Huang Y F, Li C F, Guo G C, Laine E M, Breuer H P and Piilo J 2011 *Nat. Phys.* **7** 931
[20] Yu S, Wang Y T, Ke Z J, Liu W, Meng Y, Li Z P, Zhang W H, Chen G, Tang J S, Li C F and Guo G C 2018 *Phys. Rev. Lett.* **120** 060406
[21] Ringbauer M, Wood C J, Modi K, Gilchrist A, White A G and Fedrizzi A 2015 *Phys. Rev. Lett.* **114** 090402
[22] Girolami D, Souza A M, Giovannetti V, Tufarelli T, Filgueiras J G, Sarthour R S, Soares-Pinto D O, Oliveira I S and Adesso G 2014 *Phys. Rev. Lett.* **112** 210401
[23] Dhar H S, Bera M N and Adesso G 2015 *Phys. Rev. A* **91** 032115
[24] He S, Zhang Y Y, Cheng Q H, Ren X Z, Liu T and Wang K L 2013 *Chin. Phys. B* **22** 064205
[25] Sun Z, Ma J, Wang X G and Nori F 2012 *Phys. Rev. A* **86** 012107
[26] Zheng H, Zhu S Y and Zubairy M S 2008 *Phys. Rev. Lett.* **101** 200404
[27] Xiong S J, Zhang Y, Sun Z, Yu L, Su Q P, Xu X Q, Jin J S, Xu Q J, Liu J M, Chen K F and Yang C P 2017 *Optica* **4** 1065
[28] Larson J 2012 *Phys. Rev. Lett.* **108** 033601
[29] Tanaka M and Tanimura Y 2010 *J. Chem. Phys.* **132** 214502
[30] Dijkstra A G and Tanimura Y 2010 *Phys. Rev. Lett.* **104** 250401
[31] Ishizaki A and Tanimura Y 2007 *J. Phys. Chem. A* **111** 9269
[32] Sun Z, Zhou L W, Xiao G Y, Poletti D and Gong J B 2016 *Phys. Rev. A* **93** 012121
[33] Helstrom C 1967 *Phys. Lett. A* **25** 101
[34] Helstrom C 1968 *IEEE Trans. Inform. Theory* **14** 234
[35] Braunstein S L and Caves C M 1994 *Phys. Rev. Lett.* **72** 3439
[36] Liu J, Yuan H, Lu X M and Wang X 2020 *J. Phys. A: Math. Theor.* **53** 023001
[37] Maniscalco S and Petruccione F 2006 *Phys. Rev. A* **73** 012111
[38] Wootters W K 1998 *Phys. Rev. Lett.* **80** 2245
[39] Modi K, Brodutch A, Cable H, Paterek T and Vedral V 2012 *Rev. Mod. Phys.* **84** 1655